

## P1.4 A QUANTITATIVE ANALYSIS OF THE ENHANCED-V SIGNATURE IN RELATION TO SEVERE WEATHER

Jason C. Brunner \*

Cooperative Institute for Meteorological Satellite Studies (CIMSS)/University of Wisconsin, Madison,  
Wisconsin

Steven A. Ackerman

CIMSS/University of Wisconsin, Madison, Wisconsin

A. Scott Bachmeier

CIMSS/University of Wisconsin, Madison, Wisconsin

Robert M. Rabin

National Oceanic and Atmospheric Administration (NOAA)/National Severe Storm Laboratory (NSSL),  
Norman, Oklahoma

### 1. INTRODUCTION AND BACKGROUND

Researchers have looked at enhanced-V features with 4 km spatial resolution Geostationary Operational Environmental Satellite (GOES) imagery. This paper focuses on observing enhanced-V features with higher (1 km) spatial resolution Polar Orbiting Environmental Satellite (POES) imagery, which has yet to be explored in detail. A quantitative analysis of the enhanced-V feature along with a set of enhanced-V types and a Forecasting Rules of Thumb (FRT) procedure for severe weather detection are presented in this paper.

Many studies have observed and analyzed the enhanced-V feature (McCann 1983; Negri 1982; Heymsfield et al. 1983a, 1983b; Heymsfield and Blackmer 1988; Adler et al. 1985). Enhanced longwave InfraRed (IR) satellite imagery of deep convection sometimes display this cloud-top V-shaped feature, in which an equivalent blackbody temperature (BT) region of a storm is enclosed by a V-shaped region of colder BT (see figure 1a; Negri 1982; McCann 1983; Heymsfield et al. 1983a, 1983b; Fujita 1982). The enhanced-V develops when a strong updraft penetrates into the lower stratosphere and results in an overshooting thunderstorm top. This overshooting top acts to block strong upper level winds and forces the flow to divert around it (Fujita 1978). As the flow is diverted around the

overshooting top, it erodes the updraft summit and carries cloud debris downwind (McCann 1983). The carrying of cloud debris downwind is reflected in the colder BTs of the enhanced-V feature (McCann 1983). The coldest BT, which is near the apex of the enhanced-V, is associated with adiabatic expansion due to the ascent of air parcels in the thunderstorm updraft region overshooting the tropopause (Heymsfield and Blackmer 1988; Adler and Mack 1986).

Several theories have been proposed to explain the warm region of BTs enclosed by the V-feature. One theory argues that the region is a result of subsidence of negatively buoyant overshooting cloud air downstream of an ascending cloud top (Heymsfield and Blackmer 1988; Adler and Mack 1986; Heymsfield et al., 1983a; Negri 1982; Schlesinger 1984). A second theory has been proposed which explains the warm region on the basis of radiative properties of the cloud particles. Based on radiative transfer simulations and assuming that the ice water content varied spatially across the anvil, Heymsfield et al., (1983b) suggested that the interior warm region was found to have lower ice water content compared to the V-arms. This situation implies a smaller optical depth in the warm region and warmer BTs that are characteristic of lower altitudes. Another theory states that stratospheric cirrus (Fujita 1982) generated in the wake of overshooting tops are sinking into the anvil cloud. Located above an anvil top and at a warmer environmental temperature, the stratospheric cirrus appears warmer in the BTs sensed by the IR satellite channel (Wang et al., 2002; Setvak et al., 2005).

---

*Corresponding author address:* Jason C. Brunner,  
University of Wisconsin, CIMSS, Madison, WI  
53706; e-mail: [jasonb@ssec.wisc.edu](mailto:jasonb@ssec.wisc.edu).

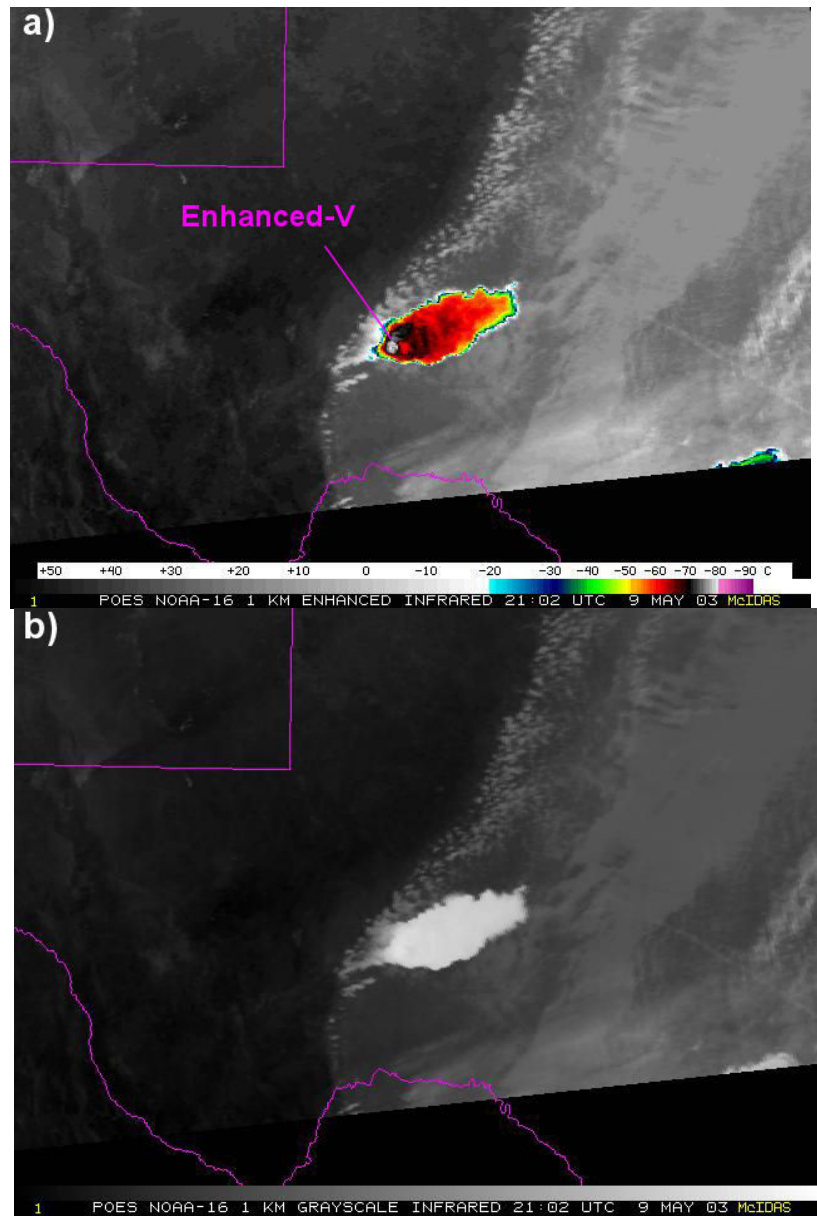


**FIGURE 1.** Deep convective storm with enhanced-V over southwestern Texas from the Polar Orbiting Environmental Satellite (POES) National Oceanic and Atmospheric Administration (NOAA) –Advanced Very High Resolution Radiometer (AVHRR) one-kilometer spatial resolution 10.8  $\mu\text{m}$  IR channel image on 9 May 2003 at 2102 UTC. (a) Color enhanced image (b) Black and white image.

Warm regions have been identified as Closed-in Warm Areas (CWA) and Distant Warm Areas (DWA) further downwind (Heymsfield et al., 1983a). The CWA and coldest point of the enhanced-V form a cold-warm couplet (McCann 1983; Heymsfield et al., 1983a, 1983b; Negri 1982; Fujita 1982). A DWA is more transient and usually has no distinct maxima of BT (Heymsfield et al., 1983a). Five Severe Environmental Storms and Mesoscale Experiment (SESAME) cases

were performed during 1979 for a GOES quantitative study of the enhanced-V (Heymsfield and Blackmer, 1988). They found that the cold-warm couplet ranged from 7 to 17° C. The distance from the cold point to the CWA was 21 to 44 km and the distance from the cold point to the DWA was 40 to 120 km. Compared to the CWA, the DWA occurred less frequently and consisted of a larger transient area when present.

The presence of enhanced-V features signifies strong tropospheric shear and intense updrafts, both of which are also essential for severe thunderstorms (Heymsfield and Blackmer 1988). The presence of enhanced-Vs is associated with severe weather (McCann 1983; Negri 1982; Heymsfield et al., 1983a, 1983b; Adler et al., 1985; Heymsfield and Blackmer 1988). McCann (1983) explored the association of enhanced-Vs to severe weather reports, suggesting their possible use in issuing severe weather warnings. McCann (1983) found a 30-minute median lead time from the time the enhanced-V appeared in enhanced IR imagery to the time of the first report of severe weather. In addition, McCann (1983) found that most of the enhanced-Vs he studied were associated with severe weather (i.e., low false alarm ratio). However, a large number of severe storms did *not* have an enhanced-V (low probability of detection).

Most of these earlier studies of enhanced-V features and their relation to severe weather have used GOES IR imagery with 8 km spatial resolution and 30-minute temporal resolution. The current GOES IR imagery has a spatial resolution of 4 km and improved temporal resolution. POES IR imagery has a spatial resolution of 1 km but with limited temporal resolution as compared to GOES imagery. A few studies have utilized POES IR imagery to investigate enhanced-V features (Adler et al., 1983). Primarily because of the coarse spatial resolution, GOES IR imagery overestimates the cold area BTs by about +15 K for mature thunderstorms and +30-40 K for small growing storms compared to POES IR imagery (Adler et al., 1983). The magnitude of the cold-warm couplet increases dramatically with POES imagery, making it easier to detect. Thus, it is expected that the number of detectable enhanced-Vs will be greater with POES imagery. To date, there has not been a detailed POES dataset of enhanced-V cases developed. This paper explores statistical categorizations between quantifiable parameters of the enhanced-V and severe weather types using a POES dataset.

Section 2 discusses the data used in this study, while Section 3 describes the methodology. Section 4 includes results including relations between quantitative parameters of the enhanced-Vs and a FRT procedure for enhanced-V features and severe weather. Conclusions are discussed in Section 5.

## 2. DATA

Two polar orbiting satellite datasets that included the 10.7, 10.8, and 11  $\mu\text{m}$  InfraRed (IR) channels were obtained over the United States of America (USA) for the enhanced-V study. These datasets consisted of:

- POES National Oceanic and Atmospheric Administration (NOAA)-Advanced Very High Resolution Radiometer (AVHRR) and Earth Observing System's (EOS) MODerate-resolution Imaging Spectroradiometer (MODIS) AQUA and TERRA overpasses from 4 May 2003 to 5 July 2003. There were 209 enhanced-V cases collected in the 2003 season.
- POES NOAA-AVHRR and EOS MODIS AQUA and TERRA overpasses from 1 May 2004 to 1 July 2004. There were 241 enhanced-V cases collected in the 2004 season.

In addition, GOES Water Vapor Derived Winds (WVDW) were used to estimate upper tropospheric winds. Archived RAdiosonde OBservations (RAOBS) were used if the GOES WVDW were not available at or near the time of the enhanced-V cases. Severe weather reports during the time periods of the enhanced-V seasons were examined.

## 3. METHODOLOGY

### 3.1 Enhanced-V in Satellite Observations

One of the goals of this enhanced-V study is to quantify aspects of the enhanced-V feature using POES observations from the AVHRR and MODIS. These satellites provide a one-kilometer spatial resolution for the 10.8 and 11  $\mu\text{m}$  IR channels. The Man computer Interactive Data Access System (McIDAS) was used to display and analyze the satellite imagery.

As mentioned in the data section, 209 enhanced-V cases were collected from 4 May 2003 to 5 July 2003 and 241 enhanced-V cases were collected from 1 May 2004 to 1 July 2004. Since each polar orbiting satellite has one ascending and one descending overpass per day at a certain location on Earth, the temporal nature of enhanced-V features is difficult to determine.

Furthermore, enhanced-V features are associated with deep convection, which usually lasts approximately a few hours. This makes enhanced-V features even more difficult to detect with polar orbiting satellites because of the “hit or miss” nature of the satellite overpasses.

For easy detection of the enhanced-V, the IR imagery is enhanced using the two-ramp dog-leg scheme for converting scene temperatures ( $T_{\text{scene}}$ ) into an unsigned 8-bit integer (count) in the range zero to 255 (Clark 1983, Brunner 2004). Refer to Figure 1b for a POES NOAA-AVHRR one-kilometer spatial resolution  $10.8 \mu\text{m}$  IR channel image of deep convection over southwestern Texas on 9 May 2003 at 2102 UTC. However, an enhanced-V feature is not evident on this black and white image. Refer to Figure 1a for the same  $10.8 \mu\text{m}$  IR channel image that was used in Figure 1b, but with the addition of the two-ramp dog-leg scheme enhancement. An enhanced-V is labeled on the enhanced IR image.

The enhanced-V has seven quantitative parameters as explained in the following paragraphs:

- TMIN
- TMAX
- TDIFF
- DIST
- DISTARMS
- ANGLEARMS
- ORIENTATION

TMIN is the minimum cloud top equivalent blackbody temperature observed from the satellite. TMIN is usually near the apex of the enhanced-V and is associated with adiabatic expansion due to the ascent of air parcels in the thunderstorm updraft region overshooting the tropopause (Heymsfield and Blackmer 1988; Adler and Mack 1986). The Latitude and Longitude for each enhanced-V case is also documented, based on the position of TMIN.

The maximum cloud top BT is TMAX. TMAX is usually observed downwind of TMIN and is enclosed by the V-feature region. Figure 2a shows a zoomed-in image of Figure 1a with TMIN and TMAX labeled. For this enhanced-V case, TMIN and TMAX were observed to have values of 192 K ( $-81^\circ \text{C}$ ) and 212 K ( $-61^\circ \text{C}$ ), respectively.

The difference in cloud top BTs between TMIN and TMAX (TDIFF) forms a cold-warm couplet (McCann 1983; Heymsfield et al., 1983a, 1983b; Negri 1982; Fujita 1982). Another quantitative parameter of the enhanced-V is the

distance between TMIN and TMAX (DIST). Figure 2b displays an enhanced-V with TDIFF and DIST applied and labeled. For this case, TDIFF and DIST were observed to have values of 20 K and 7 km, respectively.

A fifth quantitative parameter used in examining the enhanced-V set is the distance of the V-arms (DISTARMS). The V-arms extend outward in a V-like pattern from an apex point. Usually, the apex point is denoted as TMIN, and the further away from the apex of the “V”, the warmer the cloud top BTs. Sometimes, the apex of the “V” is not TMIN, but it is the coldest cloud top BT along the V-arms. DISTARMS was calculated for each enhanced-V by averaging the two V-arm distances together. The distance of each V-arm was calculated by using McIDAS to measure the distance between the apex point and the point on the V-arm where a noticeable increase in the cloud top BT occurred. This noticeable increase varied for each enhanced-V, but was roughly a 10 percent change between the temperature at the apex point and the temperature at the end of the V-arm.

ANGLEARMS is the angle between the two V-arms. Figure 2c shows DISTARMS and ANGLEARMS applied and labeled to an image; DISTARMS and ANGLEARMS were observed to have values of 22.5 km and 72 degrees, respectively.

The final quantitative descriptor, the ORIENTATION parameter, is used to describe the orientation of the enhanced-V. The ORIENTATION parameter makes four 90-degree quadrants. South was denoted as zero, or 360 degrees. Quadrant 1 (Southwest) is the angle from zero to 90 degrees (West). Quadrant 2 (Northwest) is the angle from 90 to 180 degrees (North). Quadrant 3 (Northeast) is the angle from 180 to 270 degrees (East) and Quadrant 4 (Southeast) is the angle from 270 to 360 degrees.

The quadrant(s) that each enhanced-V was assigned to is determined by two criteria. First, the quadrant that contains the highest number of degrees of the enhanced-V is counted. Second, each quadrant that contains 45 degrees or more is counted. A quadrant was not counted more than once for each enhanced-V. Figure 2d shows an example of the quantitative parameter ORIENTATION. For this enhanced-V case, the enhanced-V orientation was determined to be the northeast quadrant because there were 49 degrees of angle present in the northeast quadrant, while only 23 degrees of angle were present in the southeast quadrant.

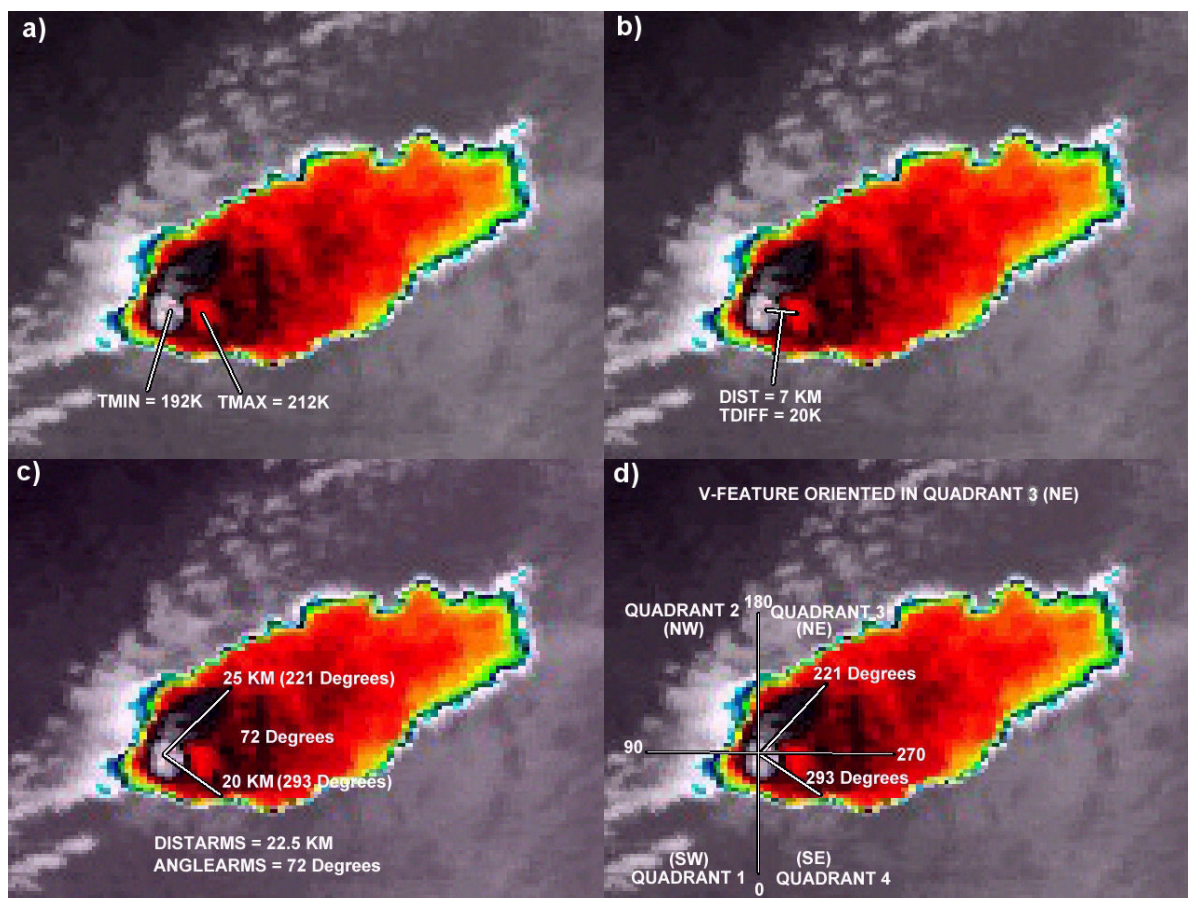


**FIGURE 2.** A zoomed-in POES NOAA-AVHRR one-kilometer spatial resolution enhanced  $10.8 \mu\text{m}$  IR channel image over southwestern Texas on 9 May 2003 at 2102 UTC. The enhanced-V quantitative parameters are labeled in the four panels (a) TMIN (K) and TMAX (K) (b) TDIFF (K) and DIST (KM) (c) DISTARMS (KM) and ANGLEARMS (Degrees), and (d) ORIENTATION.

### 3.2 Upper Level Winds

For the formation of the enhanced-V to occur, it is theorized that strong upper level winds are diverted around the overshooting thunderstorm top (Fujita 1978). In this study, upper level wind speed and direction from the GOES Water Vapor Derived Winds (WVDW) were obtained for each enhanced-V case. The GOES WVDW provide upper level winds every 30 minutes so the temporal resolution is much better than with RAOBS. Also, the horizontal spatial scale is improved with GOES WVDW. If the GOES WVDW were not available at or near the time of an enhanced-V case, then the nearest RAOB both in time and horizontal spatial scale was used instead to determine the upper level winds. For the southwestern Texas enhanced-V case discussed earlier, the upper level wind speed was estimated at 65 Knots (KT) (33 m/s) and the

upper level wind direction was towards the northeast.

### 3.3 Severe Weather Reports

Severe weather reports were also analyzed for the two enhanced-V seasons. Enhanced-V features seem to be associated more often with supercell-type thunderstorms rather than multicell-squall line thunderstorms. Consequently, for the severe weather analysis we focused on tornado and hail reports, which are more likely with supercells, rather than wind reports, which are more likely associated with squall lines. There are four categories for severe weather analysis in this study:

- Tornado and hail report
- Tornado report only
- Hail report only
- No tornado or hail report

The enhanced-V case over southwestern Texas on 9 May 2003 at 2102 UTC was assigned to the third category (hail report only). In fact, 7.6 cm (i.e., baseball) size hail was associated with this enhanced-V case.

#### 4. RESULTS

This section encompasses three main parts. First, results of the seven enhanced-V quantitative parameters are detailed. Second, the relationships between the parameters of the enhanced-V cases and the upper level winds based on the four severe weather categories are discussed. Finally, a list of enhanced-V types and a FRT procedure for enhanced-V features is included.

##### 4.1 Enhanced-V Parameters

Seven quantitative parameters of the enhanced-V cases were analyzed. Refer to Table 1 for results from both seasons for the TMIN, TMAX, TDIFF, DIST, DISTARMS, and ANGLEARMS parameters. The Mean (ME), Median (MED), Maximum (MAX), and Minimum (MIN) values of each parameter were calculated. All of the TMIN values were consistent for the 2003 and 2004 seasons. For the TMAX parameter, the MAX value of 246 K (-27° C) in the 2003 season was 14 K larger than the value for the 2004 season. Most of the TDIFF values were consistent for the two seasons except for the MAX value of 41 K for the 2004 season, which was 6 K larger than the MAX value for the 2003 season. All of the DIST values were consistent for the two seasons. Most of the DISTARMS values were consistent for the two seasons except for the MAX value of 177 km for the 2003 season, which was 30.5 km larger than the MAX value for the 2004 season. The ME and MED values for the ANGLEARMS parameter were consistent for the two seasons. However, the MAX and MIN values for the ANGLEARMS parameter were 13 degrees larger and smaller, respectively, for the 2003 season compared to the 2004 season.

The results for the ORIENTATION parameter showed that 59.8 and 72.6 percent of the time an enhanced-V was present in the northeast (number 3) quadrant, for the 2003 and 2004 seasons, respectively. Also, the results showed that 37.8 and 27.8 percent of the time an

enhanced-V was present in the southeast (number 4) quadrant, for the 2003 and 2004 seasons, respectively. The northwest (number 2) quadrant contained enhanced-Vs 9.6 and 2.9 percent of the time for the 2003 and 2004 seasons, respectively; while the southwest (number 1) quadrant contained enhanced-Vs 4.8 and 1.2 percent of the time for the 2003 and 2004 seasons, respectively. The northeast and southeast quadrants contained by far the highest percentages of enhanced-Vs, while the southwest and northwest quadrants had much smaller percentages of enhanced-Vs. For the southwest, northwest, and southeast quadrants, the percent of the time an enhanced-V was present decreased by 3.6 percent, 6.7 percent, and 10 percent, respectively, in the 2004 season compared to the 2003 season. However, for the northeast quadrant, the percent of the time an enhanced-V was present increased by 12.8 percent.

##### 4.2 Severe Weather

The distribution of the enhanced-V parameters and the upper level winds with respect to the four categories of the severe weather analysis were analyzed via a scatter diagram. There were 11 scatter diagrams from all possible combinations of the parameters that resulted in categorizations with respect to the severe weather analysis categories. One example was the TDIFF versus ANGLEARMS scatter diagram. Figures 3 and 4 show this scatter diagram for the 2003 and 2004 seasons, respectively. The severe weather analysis categories, as indicated on the scatter diagrams, are:

- Tornado and hail - blue diamond
- Tornado only – light blue “X”
- Hail only – pink box
- No tornado or hail – dark green circle

The category, No tornado or hail, indicates a false warning of severe weather. The average False Alarm Ratio (FAR), calculated from this category, was 32 percent for the enhanced-V seasons.

For the 2003 and 2004 seasons, when a TDIFF was greater than 20 K and an ANGLEARMS was greater than 71 and 72 Degrees, respectively, the storm most likely produced a tornado or hail.



**TABLE 1.** The Mean, Median, Maximum, and Minimum values for TMIN (K), TMAX (K), TDIFF (K), DIST (KM), DISTARMS (KM), and ANGLEARMS (DEGREES) for the 2003 and 2004 enhanced-V seasons.

<b>2003 SEASON:</b>				
<b>PARAMETER</b>	<b>MEAN</b>	<b>MEDIAN</b>	<b>MAXIMUM</b>	<b>MINIMUM</b>
TMIN (K)	201	200	222	184
TMAX (K)	217	217	246	205
TDIFF (K)	16	16	35	5
DIST (KM)	11	10	43	3
DISTARMS (KM)	39	31	177	9
ANGLEARMS (DEGREES)	78	75	130	25
<b>2004 SEASON:</b>				
<b>PARAMETER</b>	<b>MEAN</b>	<b>MEDIAN</b>	<b>MAXIMUM</b>	<b>MINIMUM</b>
TMIN (K)	201	201	220	181
TMAX (K)	217	217	232	206
TDIFF (K)	16	15	41	5
DIST (KM)	10	9	41	3
DISTARMS (KM)	41	34.5	146.5	10
ANGLEARMS (DEGREES)	75	74	117	38

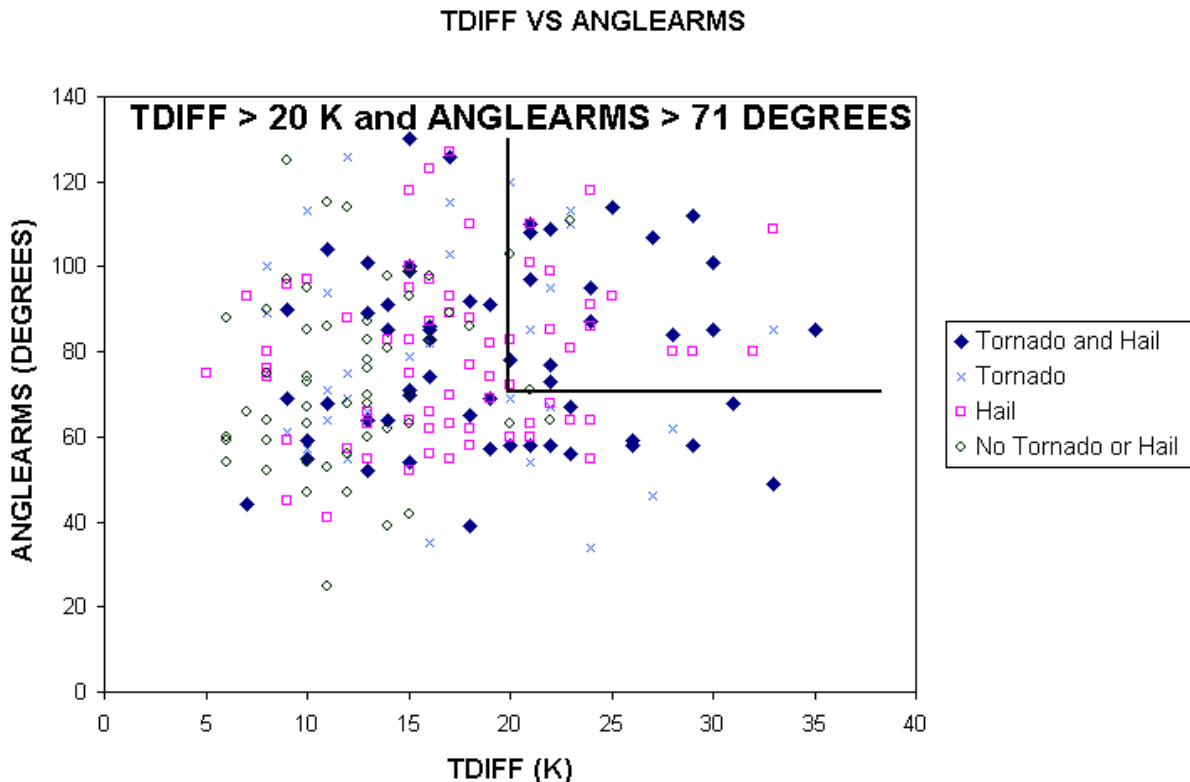


**FIGURE 3.** The TDIFF (K) VS ANGLEARMS (DEG) scatter diagram for the 2003 season. For each enhanced-V case there were four possible categories of severe weather: tornado and hail (blue diamond), tornado only (light blue "X"), hail only (pink box), and no tornado or hail (dark green circle). The lines represent a TDIFF greater than 20 K and an ANGLEARMS greater than 71 Degrees.

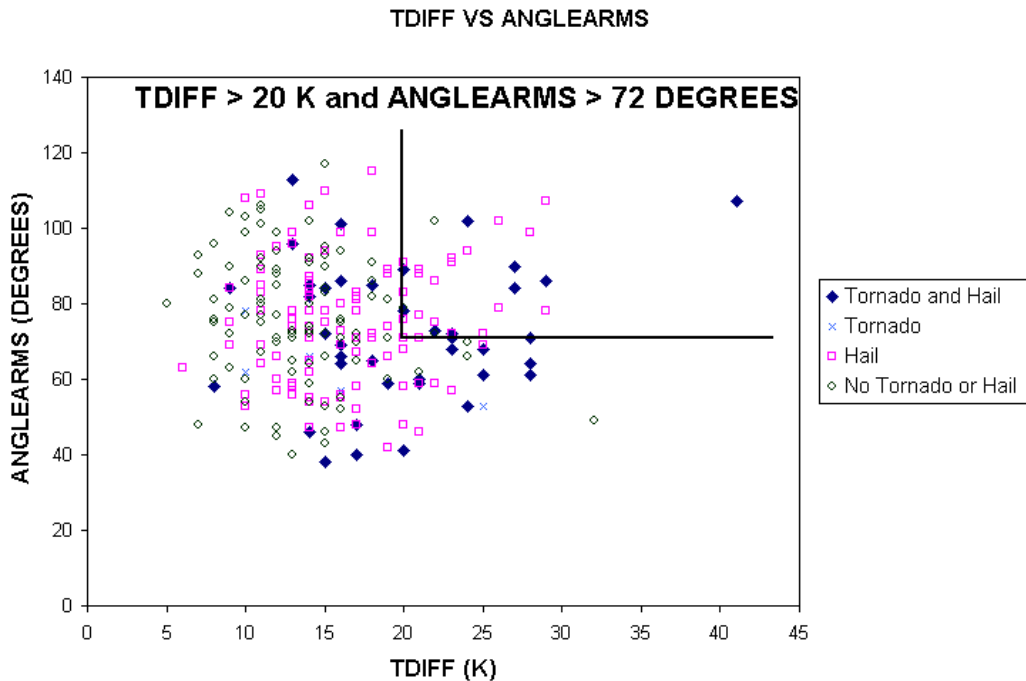


**FIGURE 4.** The TDIFF (K) VS ANGLEARMS (DEG) scatter diagram for the 2004 season. For each enhanced-V case there were four possible categories of severe weather: tornado and hail (blue diamond), tornado only (light blue “X”), hail only (pink box), and no tornado or hail (dark green circle). The lines represent a TDIFF greater than 20 K and an ANGLEARMS greater than 72 Degrees.

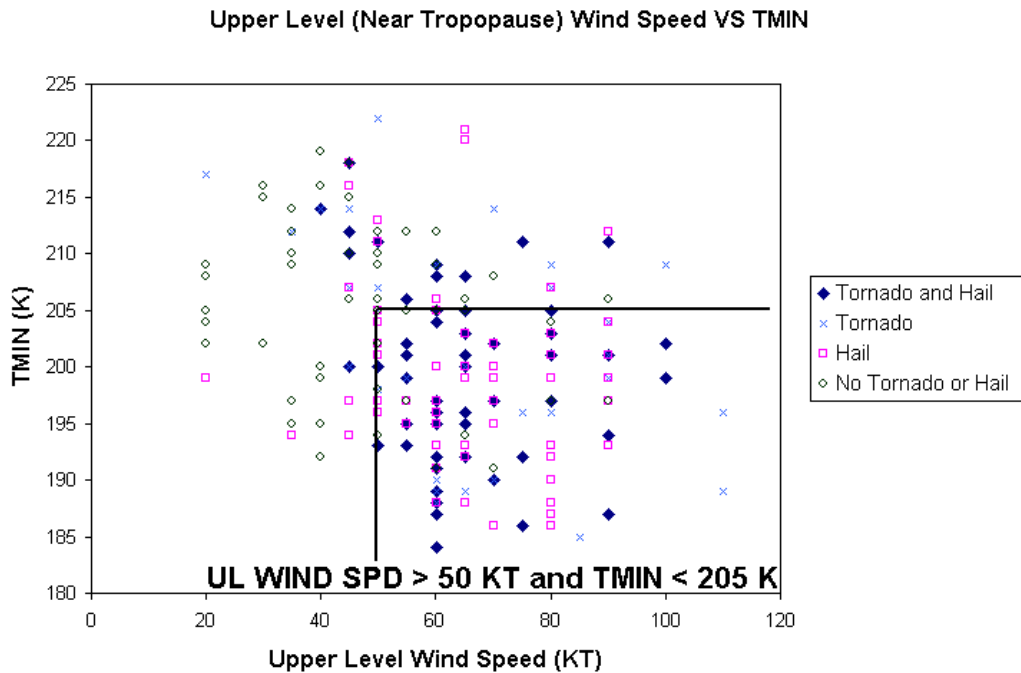


**FIGURE 5.** Same as Figure 3 but for the Upper Level (Near Tropopause) Wind Speed (UL WIND SPD) (KT) VS TMIN (K) scatter diagram for the 2003 season. The lines represent an UL WIND SPD greater than 50 KT (26 m/s) and a TMIN less than 205 K (-68° C).



Upper Level (Near Tropopause) Wind Speed VS TMIN

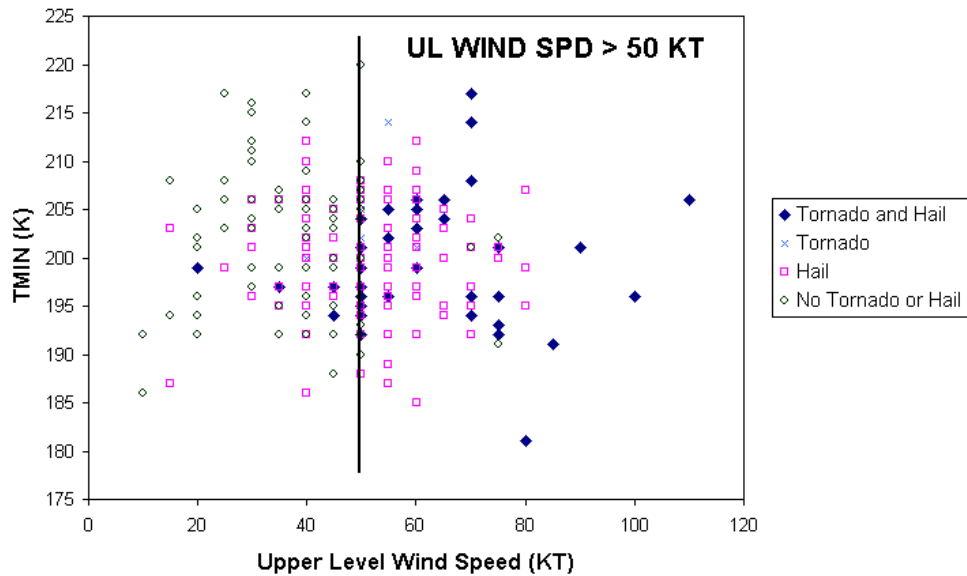


**FIGURE 6.** Same as Figure 4 but for the UL WIND SPD (KT) VS TMIN (K) scatter diagram for the 2004 season. The line represents an UL WIND SPD greater than 50 KT (26 m/s).

For the 2003 season, when the Upper Level (Near Tropopause) Wind Speed (UL WIND SPD) was greater than 50 KT (26 m/s) and TMIN was less than 205 K (-68° C), severe weather was likely to occur (Figure 5). However, TMIN did not have an impact for the 2004 enhanced-V season since the UL WIND SPD (greater than 50 KT (26 m/s)) was the only determining factor for severe weather (Figure 6).

Table 2 lists all of the categorizations between the severe weather types of tornado and/or hail and no tornado or hail for the 2003 and 2004 seasons. When the thresholds were met for each categorization, severe weather was likely.

For both seasons, there seems to be a strong correlation between the ORIENTATION parameter of the enhanced-V cases and the Upper Level (Near Tropopause) Wind Direction (UL WIND DIR) that was derived from the GOES WVDW. Assuming that a +/- 45 degree discrepancy between the two parameters is tolerated, there is an 83 percent correlation between the parameters for the 2003 season and a 90 percent correlation between the parameters for the 2004 season.

The largest number of enhanced-V cases (83 for 2003 season and 115 for 2004 season) for both seasons were oriented toward the northeast and had an UL WIND DIR toward the northeast as well. The second largest number of enhanced-V

cases (33 cases) for the 2003 season was oriented toward the southeast and had an UL WIND DIR toward the southeast as well. However, for the 2004 season, the second largest number of enhanced-V cases (39 cases) were oriented toward the northeast and had an UL WIND DIR toward the east. Overall, most of the enhanced-V cases were oriented toward the northeast or southeast because the UL WIND DIR was usually from the southwest or northwest, respectively. It can be seen from this correlation that the ORIENTATION of an enhanced-V feature can be obtained by determining the UL WIND DIR from the GOES WVDW. The UL WIND DIR could be used for pattern recognition in an enhanced-V automated detection algorithm. The WVDW could obtain the direction that the enhanced-V is oriented towards and then the algorithm could search for patterns in the equivalent blackbody temperatures.

There were a few enhanced-V cases that were outside of the tolerated degrees of discrepancy between the ORIENTATION and UL WIND DIR parameters. Most notably, in the 2003 season, there were 10 enhanced-V cases with an ORIENTATION toward the northwest and an UL WIND DIR toward the northeast (90 degree discrepancy). In addition, there were eight enhanced-V cases for the 2003 season and nine enhanced-V cases for the 2004 season with an

**TABLE 2.** The thresholds for each categorization between the severe weather types of tornado and/or hail and no tornado or hail for the 2003 and 2004 seasons.

<b>CATEGORIZATION</b>	<b>2003 SEASON</b>	<b>2004 SEASON</b>
TMIN VS TMAX	TMIN < 205 K and TMAX > 212 K	TMIN < 205 K and TMAX > 215 K
TMIN VS TDIFF	TMIN < 205 K and TDIFF > 13 K	TMIN < 207 K and TDIFF > 16 K
TMAX VS TDIFF	TDIFF > 15 K	TMAX > 216 K and TDIFF > 15 K
TMAX VS DISTARMS	TMAX > 208 K and DISTARMS > 50 KM	TMAX > 210 K and DISTARMS > 60 KM
TMIN VS DISTARMS	TMIN < 202 K and DISTARMS > 35 KM	TMIN < 201 K and DISTARMS > 40 KM
TDIFF VS DIST	TDIFF > 15 K and DIST < 20 KM	TDIFF > 18 K and DIST < 20 KM
TDIFF VS DISTARMS	TDIFF > 14 K and DISTARMS > 51 KM	TDIFF > 15 K and DISTARMS > 67 KM
TDIFF VS ANGLEARMS	TDIFF > 20 K and ANGLEARMS > 71 DEGREES	TDIFF > 20 K and ANGLEARMS > 72 DEGREES
DIST VS DISTARMS	DIST < 18 KM and DISTARMS > 49 KM	DIST < 18 KM and DISTARMS > 63 KM
UL WIND SPD VS TMIN	UL WIND SPD > 50 KT (26 M/S) and TMIN < 205 K	UL WIND SPD > 50 KT (26 M/S)
UL WIND SPD VS TDIFF	UL WIND SPD > 40 KT (21 M/S) and TDIFF > 15 K	UL WIND SPD > 50 KT (26 M/S)

ORIENTATION toward the southeast and an UL WIND DIR toward the northeast (90 degree discrepancy). There were also nine cases in the 2004 season with an ORIENTATION toward the northeast and an UL WIND DIR toward the southeast (90 degree discrepancy). It is not known why these 90 degree discrepancies occurred, but there seem to be other processes beyond the UL WIND DIR that determines the ORIENTATION of an enhanced-V case. However, in general the UL WIND DIR is a good indicator of the ORIENTATION of an enhanced-V case.

#### **4.3 Enhanced-V Types and FRT**

Eleven enhanced-V types were defined based on the satellite-derived parameters developed from the scatter diagrams discussed above. For each enhanced-V type, two parameter thresholds must be met. Table 3 lists these enhanced-V types and thresholds needed for each type. The eleven types are listed alphabetically from Type A to Type K. An enhanced-V feature

can have one enhanced-V type, multiple enhanced-V types, or no enhanced-V types.

All of the enhanced-V cases from both seasons were analyzed for type. A Type B enhanced-V was the most prevalent in both seasons (50.5 percent average). The enhanced-V types A (41.5 percent), J (37.5 percent), K (37.5 percent), and F (36 percent) had the next highest average percentages. Enhanced-V types C (29.0 percent), E (23.5 percent), D (19.0 percent), and G (15.0 percent) had lower average percentages. The enhanced-V types H and I (both 13.5 percent) had the lowest average percentages of all types. There were no enhanced-V types seen for about 31 percent of the cases from the seasons.

Table 4 lists the percentage of enhanced-V cases from both seasons that had a certain number of enhanced-V types associated with them. The number of types assigned ranges from one to eleven. The largest average percentage (12.5 percent) for the number of types assigned was for one enhanced-V type, and the smallest average percentage (0.7 percent) was for all of the enhanced-V types. Generally, as the number of

**TABLE 3.** The enhanced-V types and the thresholds for each enhanced-V type. For each type there are two thresholds that need to be met in order for an enhanced-V feature to be classified under that type.

Enhanced-V Type	THRESHOLDS NEEDED TO BE MET
A	TMIN < 205 K and TMAX > 213.5 K
B	TMIN < 206 K and TDIFF > 14.5 K
C	TDIFF > 15 K and TMAX > 216 K
D	TMAX > 209 K and DISTARMS > 55 KM
E	TMIN < 201.5 K and DISTARMS > 37.5 KM
F	TDIFF > 16.5 K and DIST < 20 KM
G	TDIFF > 14.5 K and DISTARMS > 59 KM
H	TDIFF > 20 K and ANGLEARMS > 71.5 DEGREES
I	DIST < 18 KM and DISTARMS > 56 KM
J	UL WIND SPD > 50 KT (26 M/S) and TMIN < 205 K
K	UL WIND SPD > 45 KT (23 M/S) and TDIFF > 15 K

**TABLE 4.** The percentage of enhanced-V cases from both seasons that had a certain number of enhanced-V types associated with them.

Number of Enhanced-V Types	2003 Season Percent	2004 Season Percent
1	9	16
2	7	10
3	6	7
4	5	8
5	13	7
6	9	5
7	9	7
8	3	5
9	2	2
10	4	3
11	1	0.4

enhanced-V types assigned increased, the percentages decreased.

The enhanced-V cases that were classified as certain enhanced-V types were analyzed to determine if they were associated with hail and/or a tornado. Table 5 lists the percentage of cases from both seasons that were classified under each enhanced-V type and had hail and/or a tornado associated with them. In addition, the percentage of cases that were not classified as an enhanced-V type but had hail and/or a tornado associated with them (Category NONE) is shown. The largest average percentages were from enhanced-V types H (94.5 percent), J (94 percent), and K (94 percent). Therefore, these three types were the most reliable in terms of associating hail and/or a tornado with them. Specifically, Type H enhanced-Vs focus on a large TDIFF (greater than 20 K) and the ANGLEARMS (greater than 71.5 degrees) parameter. The temperature couplet between TMIN and TMAX seems to be one of the best indicators of hail and/or a tornado potential with enhanced-V cases.

Type J enhanced-Vs focus on strong UL WIND SPDs (greater than 50 KT (26 m/s)) and colder TMIN (less than 205 K), while Type K enhanced-Vs focus on strong UL WIND SPDs (greater than 45 KT (23 m/s)) and fairly large TDIFF (greater than 15 K). The UL WIND SPD seems to be another critical indicator of hail and/or tornado potential with enhanced-V cases. The TMIN and TDIFF parameters, in conjunction with the UL WIND SPD, seem to play roles as well. Even the smallest average percentages from enhanced-V Types A and E (85 percent for both) are still reasonably well associated with hail and/or a tornado. If a case is classified as at least one enhanced-V type, then it is most likely associated with hail and/or a tornado as well. Therefore, there is severe weather forecasting potential with these enhanced-V types. It is worth noting, however, if a case is not classified as an enhanced-V type, then it is still possible to have hail and/or a tornado associated with it. The average percentage of cases that were not classified as an enhanced-V type but had hail

**TABLE 5.** The percentage of enhanced-V cases from both seasons that were classified under each enhanced-V type and had hail and/or a tornado associated with them. In addition, the percentage of enhanced-V cases that were not classified as an enhanced-V type but had hail and/or a tornado associated with them (Category NONE) is shown.

Enhanced-V Type	2003 Season Percent	2004 Season Percent
A	94	76
B	95	74
C	97	86
D	95	77
E	90	80
F	94	84
G	97	84
H	97	92
I	100	78
J	93	95
K	96	92
NONE	47	37

**TABLE 6.** The percentage of enhanced-V cases from both seasons that had a certain number of enhanced-V types and hail and/or a tornado associated with them.

Number of Enhanced-V Types	2003 Season Percent	2004 Season Percent
1	61	54
2	80	58
3	67	65
4	80	74
5	96	69
6	95	91
7	100	94
8	100	92
9	100	100
10	100	100
11	100	100

and/or a tornado associated with them (Category NONE) was approximately 42 percent.

Table 6 lists the percentage of enhanced-V cases from both seasons that had a certain number of enhanced-V types and hail and/or a tornado associated with them. The largest average percentages were for enhanced-V cases that had nine, 10, and 11 enhanced-V types (100 percent for all three). The smallest average percentage (57.5 percent) was for enhanced-V cases that had one enhanced-V type. Generally,

as the number of enhanced-V types increased for the cases, the percentages increased as well. Therefore, an increase in the number of types for a case can lead to a higher likelihood of hail and/or a tornado associated with it. Even with a case that is classified as having just one enhanced-V type, there is still an above average chance (57.5 percent averaged) hail and/or a tornado is associated with it.

The main points developed in the last few paragraphs can be summarized into a FRT procedure:

- STEP 1 – An enhanced-V case is first classified as one enhanced-V type, multiple enhanced-V types, or no enhanced-V types (see Table 3).
- STEP 2 – Certain enhanced-V types have a higher likelihood that they are associated with hail and/or a tornado compared to other enhanced-V types. For example, types H, J, and K (see Table 5) have the highest likelihood (94.5 percent, 94 percent, and 94 percent, respectively), while types A and E have the smallest likelihood (85 percent for both).
- STEP 3 – If an enhanced-V case is classified as multiple enhanced-V types, then there is even a higher likelihood that the enhanced-V case is associated with hail and/or a tornado (i.e., it is more likely than a case classified as one enhanced-V type) (see Table 6).
- STEP 4 – If an enhanced-V case is not classified as an enhanced-V type, then the likelihood that the enhanced-V case is associated with hail and/or a tornado is less compared to an enhanced-V case that is classified as an enhanced-V type. However, there is still the possibility that an enhanced-V case that is not classified as an enhanced-V type is associated with hail and/or a tornado (42 percent chance).

## 5. CONCLUSIONS

With regards to severe weather categories, eleven enhanced-V types were developed from relationships of the parameters defining the enhanced-V feature and upper level winds. From these enhanced-V types, a Forecasting Rules of Thumb procedure was developed. In addition, the False Alarm Ratio was 32 percent (averaged) for the 2003 and 2004 enhanced-V seasons. The False Alarm Ratio for detecting tornadoes with the Weather Surveillance

Radar 88 Doppler (WSR-88D) is much higher at 76 percent (Simmons and Sutter, 2005), which shows an advantage of using enhanced-V features from satellite imagery for severe weather detection in addition to radar-based algorithms.

The Upper Level Wind Direction and Upper Level Wind Speed can be obtained from the GOES WVDW. These WVDW provide a temporal scale of every half hour compared to Radiosonde Observations (RAOBs), which occur twice per day. Also, the spatial scale is usually better with the WVDW compared to RAOBs. The UL WIND DIR could be used for pattern recognition in an enhanced-V automated detection algorithm. The WVDW could obtain the direction that the enhanced-V is oriented towards and then the algorithm could search for patterns in the equivalent blackbody temperatures.

The enhanced-V types and FRT procedure developed in this study focused on using one-kilometer spatial resolution polar orbiting satellite imagery. It seems plausible that these enhanced-V types and FRT procedure could be applied to the upcoming GOES ABI with its two-kilometer spatial resolution (Schmit et al., 2004). In contrast, most likely the current GOES four-kilometer spatial resolution imagery has too coarse of a resolution to use the enhanced-V types and FRT procedure developed for this research. A similar methodology could be used to investigate if a GOES four-kilometer spatial resolution FRT procedure for enhanced-V features is feasible. While the GOES ABI will not have the same spatial resolution as polar orbiting satellite imagery, the two-kilometer spatial resolution will be an improvement from the current four-kilometer GOES satellite imagery and the temporal resolution will be superior to that of polar orbiting satellites. The spatial resolution of polar orbiting satellite imagery and the improved spatial resolution of the upcoming GOES ABI allow a detailed quantitative study of the enhanced-V feature.

The enhanced-V feature from satellite imagery should be used in a severe weather warning detection algorithm along with other methods/instruments, such as radar. It should not be used as a stand-alone feature only. Warning decision making for severe weather should incorporate satellite imagery in the future, which has not occurred in many past studies (Andra et al., 2002). While radar is arguably the primary warning decision tool for severe convection, there are times when radar is either unavailable (outages) or ambiguous (for example, beam

blockage). Satellite data should certainly be used to add confidence to the radar signatures (with their high false alarm ratios), especially for severe storms whose distance from the radar is great (or increasing).

*Acknowledgements.* The archived POES NOAA-AVHRR overpasses were obtained from the Satellite Active Archive (SAA) and archived EOS MODIS AQUA and TERRA overpasses were obtained from the Goddard Space Flight Center (GSFC) Distributed Active Archive Center (DAAC). GOES WVDW were provided by Bob Rabin at the Cooperative Institute for Meteorological Satellite Studies (CIMSS) at UW-Madison. These upper level wind speeds and directions were estimated from the automated satellite winds algorithm developed at CIMSS. Archived RAOBS were obtained from the Department of Atmospheric Science at the University of Wyoming. The Storm Data Publication (SDP) from the National Climatic Data Center (NCDC) was used for analyzing storm reports for the 2003 enhanced-V season. The preliminary storm reports from the Storm Prediction Center (SPC) were used for the 2004 enhanced-V season. This is because the SDP from the NCDC was not available at the time of the analysis of storm reports for the 2004 season.

## REFERENCES

- Adler, R. F., and R. A. Mack, 1986: Thunderstorm cloud top dynamics as inferred from satellite observations and a cloud top parcel model. *Journal of Atmospheric Science*, **43**, 1945-1960.
- Adler, R. F., M. J. Markus, and D. D. Fenn, 1985: Detection of severe Midwest thunderstorms using geosynchronous satellite data. *Monthly Weather Review*, **113**, 769-781.
- Adler, R. F., M. J. Markus, D. D. Fenn, G. Szejwach, and W. E. Shenk, 1983: Thunderstorm top structure observed by aircraft overflights with an infrared radiometer. *Journal of Applied Meteorology*, **22**, 579-593.
- Andra, D. L., Jr., E. M. Quetone, and W. F. Bunting, 2002: Warning Decision Making: The Relative Roles of Conceptual Models, Technology, Strategy, and Forecaster Expertise on 3 May 1999. *Weather and Forecasting*, **17**, 559-566.
- Brunner, J. C., 2004: *A Quantitative Analysis Of The Enhanced-V Feature In Relation To Severe Weather*. M. S. thesis, Dept. of Atmospheric and

Oceanic Sciences, University of Wisconsin-Madison, 96 pp.

Clark, J. D. (ed.), 1983: *The GOES User's Guide*. U.S. Dept. of Commerce, Washington D.C.

Fujita, T. T., 1978: Manual of downburst identification for Project NIM-ROD. SMRP 156, University of Chicago, 104 pp.

Fujita, T. T., 1982: Principle of stereoscopic height computations and their applications to stratospheric cirrus over severe thunderstorms. *Journal of Meteorological Society of Japan*, **60**, 355-368.

Heymsfield, G. M., and R. H. Blackmer, Jr., 1988: Satellite-observed characteristics of Midwest severe thunderstorm anvils. *Monthly Weather Review*, **116**, 2200-2224.

Heymsfield, G. M., and R. Fulton, 1994: Passive microwave structure of severe tornadic storms on 16 November 1987. *Monthly Weather Review*, **122**, 2587-2595.

Heymsfield, G. M., R. H. Blackmer, Jr., and S. Schotz, 1983: Upper level structure of Oklahoma tornadic storms on 2 May 1979, Pt. 1 radar and satellite observations. *Journal of Atmospheric Science*, **40**, 1740-1755.

Heymsfield, G. M., G. Szejwach, S. Schotz, and R. H. Blackmer, Jr., 1983: Upper level structure of Oklahoma tornadic storms on 2 May 1979, Pt. 2 Proposed explanation of "V" pattern and internal warm region in infrared observations. *Journal of Atmospheric Science*, **40**, 1756-1767.

Homar, V., M. Gaya, and C. Ramis, 2001: A synoptic and mesoscale diagnosis of a tornado outbreak in the Balearic Islands. *Atmospheric Research*, **56**, 31-55.

Levizzani, V., and M. Setvak, 1996: Multispectral, high-resolution satellite observations of plumes on top of convective storms. *Journal of Atmospheric Science*, **53**, 361-369.

Mack, R. A., A. F. Hasler, and R. F. Adler, 1983: Thunderstorm cloud top observations using satellite stereoscopy. *Monthly Weather Review*, **111**, 1949-1964.

McCann, D. W., 1983: The enhanced-V: A satellite observable severe storm signature. *Monthly Weather Review*, **111**, 887-894.

Negri, A. J., 1982: Cloud-top structure of tornadic storms on 10 April 1979 from rapid scan and stereo satellite observations. *Bulletin of the American Meteorological Society*, **63**, 1151-1159.

Scanlon, R. J., 1987: *Mesoscale application of high resolution imagery*. M. S. thesis, Dept. of The Navy, Naval Postgraduate School, 133 pp.

Schlesinger, R. E., 1984: Mature thunderstorm cloud-top structure and dynamics: A three-dimensional numerical simulation study. *Journal of Atmospheric Science*, **41**, 1551-1570.

Schlesinger, R. E., 1988: Effects of stratospheric lapse rate on thunderstorm cloud-top structure in a three-dimensional numerical simulation, Pt. 1, Some basic results of comparative experiments. *Journal of Atmospheric Science*, **45**, 1555-1570.

Schmit, T. J., M. M. Gunshor, W. P. Menzel, J. Li, S. Bachmeier, and J. J. Gurka, 2004: Introducing the Next-generation Advanced Baseline Imager (ABI) on Geostationary Operational Environmental Satellites (GOES)-R, Submitted to the *Bulletin of the American Meteorological Society*.

Setvak, M., R. M. Rabin, and P. K. Wang, 2005: Contribution of MODIS instrument to the observations of deep convective storms and stratospheric moisture detection in GOES and MSG imagery. *Atmospheric Research (submitted in March 2005; accepted for press in September 2005)*.

Setvak, M., R. M. Rabin, C. A. Doswell III, and V. Levizzani, 2003: Satellite observations of convective storm tops in the 1.6, 3.7, and 3.9  $\mu\text{m}$  spectral bands. *Atmospheric Research*, **67**, 607-627.

Simmons, K. M., and D. Sutter, 2005: WSR-88D Radar, Tornado Warnings, and Tornado Casualties. *Weather and Forecasting*, **20**, 301-310.

Wang, P. K., H-m. Lin, S. Natali, S. Bachmeier, and R. Rabin, 2002: Cloud model interpretation of the mechanisms responsible for the satellite-observed enhanced V and other features atop some Midwest severe thunderstorms. *Proceedings*



*of the 11<sup>th</sup> American Meteorological Society  
Conference on Cloud Physics, Ogden, UT, June  
3-7, 2002.*